Journal of Power Sources 219 (2012) 45–51

Contents lists available at SciVerse ScienceDirect

Journal of Power Sources

journal homepage: www.elsevier.com/locate/jpowsour

A new hydrothermal synthesis of spherical $Li_4Ti_5O_{12}$ anode material for lithium-ion secondary batteries

Hui Yan [a], Zhi Zhu [a], Ding Zhang [b], Wei Li [c], Qilu [a,*]

[a] New Energy Materials and Technology Laboratory, Institute of Applied Chemistry, College of Chemistry and Molecular Engineering, Peking University, Beijing 100871, PR China
[b] Department of Applied Chemistry, College of Chemistry and Chemical Engineering, Taiyuan University of Technology, Taiyuan 030024, PR China
[c] School of Materials Science and Engineering, University of Science and Technology Beijing, Beijing 100083, PR China

HIGHLIGHTS

- A simple and convenient hydrothermal synthesis method to prepare $Li_4Ti_5O_{12}$.
- Several key parameters of hydrothermal synthesis method are concretely investigated.
- Precursor can be heated directly to prepare the $Li_4Ti_5O_{12}$ without any treatment.
- High tap density and controllable morphology spherical spinel $Li_4Ti_5O_{12}$ materials.
- Spherical spinel $Li_4Ti_5O_{12}$ materials show excellent electrochemical performance.

GRAPHICAL ABSTRACT

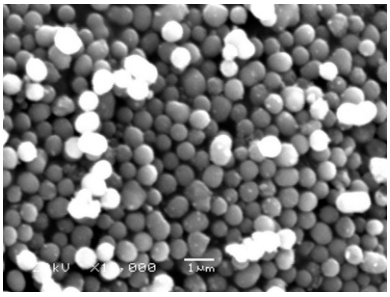

ARTICLE INFO

Article history:
Received 11 May 2012
Received in revised form
9 July 2012
Accepted 11 July 2012
Available online 21 July 2012

Keywords:
Lithium-ion secondary batteries
Lithium titanate
Spherical
Hydrothermal synthesis

ABSTRACT

As-prepared anatase TiO_2 with different particle sizes are heated in a lithium hydroxide solution to form Li–Ti–O precursors by using hydrothermal method. Spherical $Li_4Ti_5O_{12}$ powders with different particle sizes are obtained by calcining the precursors at 800 °C. The X-ray diffraction (XRD) indicates that elevated hydrothermal reaction temperature and higher concentration of lithium hydroxide solution eliminate the content of impurity in the final product. Scanning electron microscopy (SEM) shows the obtained powders have regular spherical morphology. The obtained $Li_4Ti_5O_{12}$ with particle size of about 0.5 μm exhibits excellent electrochemical performance, and the initial discharge capacity reaches 165 mAh g^{-1} at 35 mA g^{-1} (0.2 C) and more than 97% of the initial capacity is retained after 70 cycles.

1. Introduction

Graphite/carbon-related materials have been widely applied as anode in lithium-ion secondary batteries for mobile phones, digital cameras, laptops and other digital products. However, these state-of-the-art lithium-ion secondary batteries composed of a graphite/carbon related anode have shown low discharge capacity, poor cycle and calendar life, moreover, it may cause combustion or explosion at elevated temperatures during the high rate charging/discharging process [1–5]. Thus, it impedes the application in electric vehicles (EVs) and electric energy storage devices which need rapid charge/discharge and high safety.

Researchers have tried to seek alternative anode materials for carbon materials, and in a variety of alternative materials, such as

* Corresponding author. Tel.: +86 10 62751000; fax: +86 10 62755290.
E-mail addresses: qilu@pku.edu.cn, tdg@pku.edu.cn (Qilu).

0378-7753/$ – see front matter © 2012 Elsevier B.V. All rights reserved.
http://dx.doi.org/10.1016/j.jpowsour.2012.07.023

MO (M = Cu, Co, Ni, Fe, Sn), LiMN (M = Cu, Co, Ni), alloy [6–9], spinel $Li_4Ti_5O_{12}$ is considered to be promising for high-power lithium-ion secondary batteries [10–15]. Although $Li_4Ti_5O_{12}$ has an extreme flat operation potential plateau at about 1.55 V vs. Li^+/Li which results in low energy density, it could be well used in most of electrolyte systems. Its stable oxide structure could ensure superior cycle stability and security during the rapid charging/discharging process.

Generally, $Li_4Ti_5O_{12}$ has mainly been synthesized by a solid state reaction of stoichiometric amounts of TiO_2 and Li_2CO_3 or LiOH (often >850 °C and >12 h) [5,16–19]. Such process is simple but difficult to provide qualified $Li_4Ti_5O_{12}$, for the morphology and homogeneous particle size distribution significantly limit the electrochemical performance. Some researchers have reported wet chemical synthesis methods to obtain nano-sized $Li_4Ti_5O_{12}$ particles [20–26], such as sol–gel, microemulsion and spray pyrolysis. However, nano-materials have a very high surface area and inferior tap density [20,21,27]. According to the research reported by Arico [28], high surface area implies higher reactivity and thus leads to deactivation of the active mass at a faster rate accompanied with rapid capacity decay. Amine [29] considered that the lower tap density results in low energy density of the battery and therefore it cannot well meet the energy requirement for energy storage devices.

In various wet chemical synthesis methods, hydrothermal reaction method has been tried to prepare $Li_4Ti_5O_{12}$ [30–32]. However, the adoption of organic reagents as raw materials and subsequent complicated washing processes cause a lot of trouble. Also, expensive and highly toxic organic reagents limit the mass production. In order to solve the problems in mentioned above, we reported a facile hydrothermal technique to prepare $Li_4Ti_5O_{12}$ which shows excellent charging/discharging capacity, cycling stability and high rate performance. This hydrothermal method that is superior for inorganic titanium salt has favorable solubility in water, and a uniform Li–Ti–O precursor which is easy to obtain [33].

In order to obtain the $Li_4Ti_5O_{12}$ with high tap density, homogeneous particle size distribution and excellent charging/discharging performance, the effects of two kinds of TiO_2 crystal structures, hydrothermal reaction temperature, hydrothermal reaction time and lithium hydroxide alkali solution concentration on the structure and morphology of $Li_4Ti_5O_{12}$ were concretely investigated in this paper, respectively. Based on several key parameters of hydrothermal method research, spherical $Li_4Ti_5O_{12}$ powders with different particle size were synthesized and its electrochemical performance was also discussed. The process of the hydrothermal reaction and solid state reaction was also studied in detail.

2. Experimental

2.1. Synthesis of $Li_4Ti_5O_{12}$

Firstly, titanium (IV) sulfate ($Ti(SO_4)_2$, 99.5%, Sinopharm Chemical Reagent Co., Ltd., China) was dissolved in deionized water at room temperature to get 0.8 M $Ti(SO_4)_2$ solution. This aqueous solution was mixed with n-propyl alcohol (n-PrOH 99.7%, Beijing Yili Fine Chemicals Co., Ltd., China) and stirred for 5 min. The volume ratio of n-PrOH to $Ti(SO_4)_2$ solution was set at 1.0. Polyvinglpyrrolidone (PVP, molecular weight = 30,000, Beijing Chemical Reagent Company, China) was used as the dispersant for the above solution. The prepared solution was kept in an isothermal water bath at 80 °C without stirring and the yielded sub-microsized spherical TiO_2 was used as titanium source for synthesizing $Li_4Ti_5O_{12}$.

Secondly, lithium hydroxide ($LiOH\cdot H_2O$, Xilong Chemical Co. Ltd., China) was dissolved in deionized water at room temperature to obtain 5 M LiOH solution. As-prepared TiO_2 mixed with the LiOH solution and the mixture was transferred into a Teflon-lined autoclave to heat at 100 °C for 20 h, without any shaking or stirring. In a previous work [33], it had been clearly discussed the effect of sintered temperature on the structure, morphology and electrochemical performance of the $Li_4Ti_5O_{12}$; the obtained Li–Ti–O precursor here is sintered at 800 °C for 2 h in a muffle furnace under air atmosphere to get the final white products.

2.2. Cell fabrication

The coin-type cell (LIR2032) was based on the configuration of Li metal (−) |electrolyte| $Li_4Ti_5O_{12}$ (+). The synthesized $Li_4Ti_5O_{12}$, carbon black and polyvinylidene fluoride (PVdF) were mixed in a weight ratio of 90:4:6, respectively, and then were mixed in *N*-Methyl pyrrolidone (NMP) solvent to form homogeneous slurry. The slurry was coated on an Al foil current collector, and dried at 120 °C for 24 h to remove the solvent. The electrodes were punched to be a disk with a diameter of 14 mm for the half-cell test. The electrolyte solution was 1 M $LiPF_6$ dissolved in a mixture of ethylene carbonate (EC), dimethyl carbonate (DMC) and ethyl methyl carbonate (EMC) (volume ratio is 1:1:1). Microporous polypropylene film (Celgard, 2400) was used as the separator. The cells assembly was carried out in a glove box (MBRAUN, Germany) filled with pure argon for electrochemical tests.

2.3. Characterization

The crystal structures of the obtained white powders were examined by X-ray diffraction (XRD, Rigaku, D/max-2500, Japan) with Cu Kα radiation. The diffraction patterns were recorded at room temperature in the 2θ range from 10 to 90° with a scanning step of 4° min^{-1}. The surface morphology of the powders was observed by scanning electron microscopy (SEM, JSM-5600LV, Japan). The Brunauer–Emmet–Teller (BET) surface areas of three samples with different particle sizes were measured by high-speed gas sorption analyzer (ASAP 2010, MICROMETER, USA). Prior to measure the specific surface area, the materials were dried at 120 °C for 24 h under vacuum. The molecular spectroscopy of raw materials, precursors and products were identified by Fourier transform infrared spectroscopy (FTIR-8400, SHIMADZU, Japan) using a KBr method. The thermo gravimetric (TG) of the precursors was performed on a TGA thermal analyzer (TG-DSC 131, SETARAM, France). The TG curve was recorded in a static atmosphere at a heating rate of 10 °C min^{-1} from room temperature to 900 °C.

The cells were cycled under different charge/discharge rate (0.2 C, 35 mA g^{-1} to 2 C, 350 mA g^{-1}) between 2.5 and 1.0 V on a multi-channel battery test system (LAND CT2001A, Wuhan Jinnuo Electronics Co., Ltd.) at room temperature.

3. Results and discussion

3.1. Effects of two kinds of TiO_2 crystal structures on $Li_4Ti_5O_{12}$ product

The effect of TiO_2 crystal structures on the structure of $Li_4Ti_5O_{12}$ has been studied. Two kinds of TiO_2 with different crystal structures, anatase TiO_2 (as-prepared) and rutile TiO_2 (Shanghai Yuejiang Titanium Chemical Manufacturer Co., Ltd., China), are used as the reactants. Fig. 1a and b shows the XRD patterns of the reactants, precursors and yielded $Li_4Ti_5O_{12}$, respectively. Fig. 1a indicates that when anatase TiO_2 is used, the obtained precursor from the hydrothermal reaction is a mixture of TiO_2 and Li–Ti–O, and the

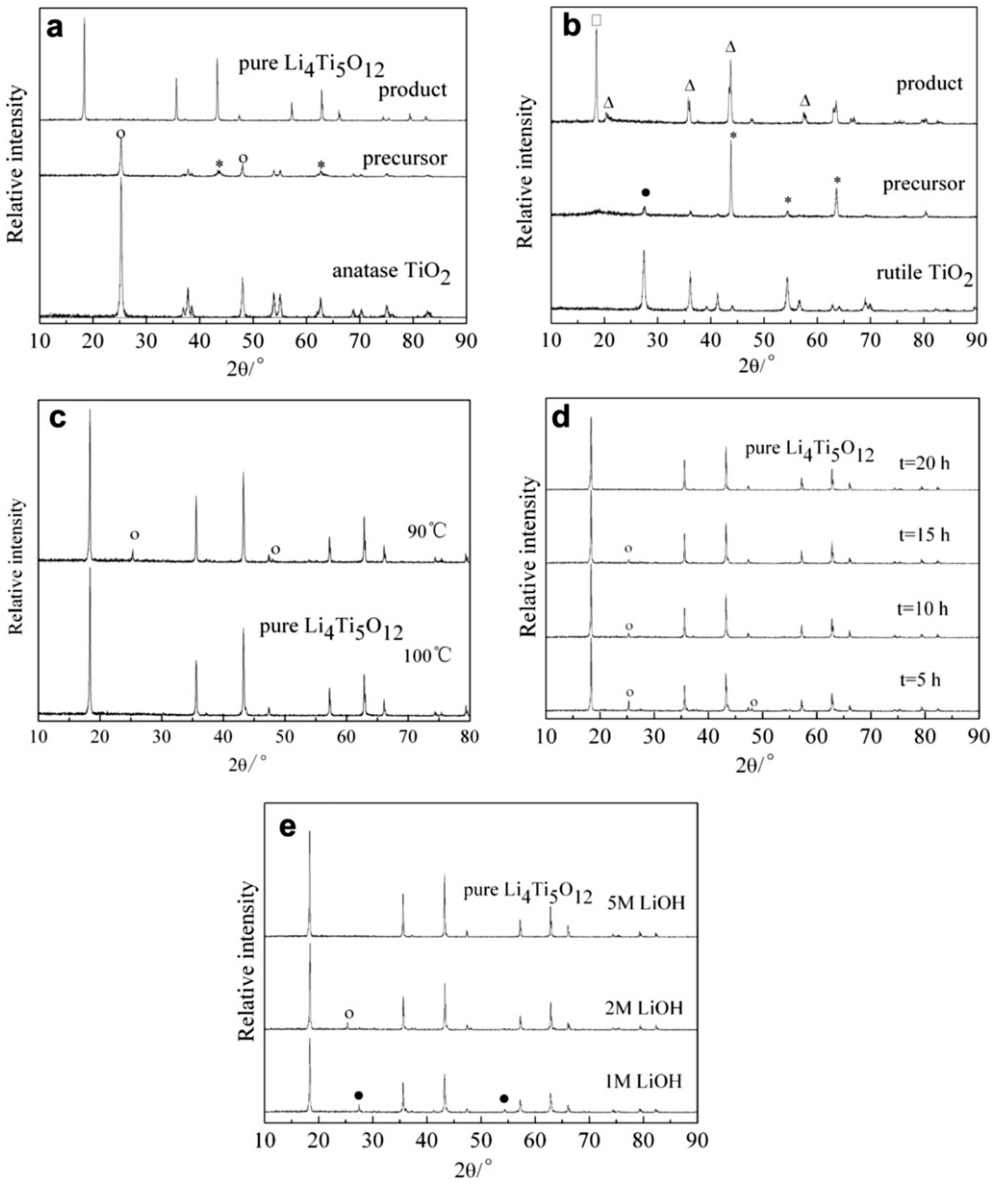

Fig. 1. XRD patterns of the samples by (a) anatase TiO_2 after the hydrothermal reaction, (b) rutile TiO_2 after the hydrothermal reaction, (c) calcining the precursor obtained in LiOH solution at different hydrothermal temperature, (d) calcining the precursor obtained at different hydrothermal time and (e) calcining the precursor obtained in different LiOH solution with 4:5 of Li/Ti at 800 °C, respectively (○: anatase TiO_2, ●: rutile TiO_2, △: Li_2TiO_3, *: Li–Ti–O, □: $Li_4Ti_5O_{12}$).

final product is pure $Li_4Ti_5O_{12}$. When rutile TiO_2 is used as the reactants, as shown in Fig. 1b, the formed precursor under the same hydrothermal reaction condition is mainly Li–Ti–O and minor unreacted TiO_2. And the final product is mainly Li_2TiO_3, only containing a small ratio of $Li_4Ti_5O_{12}$. The presence of monoclinic Li_2TiO_3 in prepared $Li_4Ti_5O_{12}$ significantly depresses the electrochemical performance [34]. Compared with rutile TiO_2, anatase TiO_2 is readily to transform into $Li_4Ti_5O_{12}$ by the hydrothermal reaction method. Thus, as-prepared anatase TiO_2 is used to prepare the $Li_4Ti_5O_{12}$ for the following research.

3.2. Effects of hydrothermal reaction temperature and time on $Li_4Ti_5O_{12}$ product

Fig. 1c shows the XRD patterns of final products obtained by as-prepared TiO_2 in LiOH solution at 90 °C and 100 °C, respectively. When the hydrothermal temperature is set at 90 °C, the impurity peaks of TiO_2 (rutile and anatase) in product are clearly observed. In contrast, the peaks of TiO_2 cannot be detected completely on the condition of 100 °C. Some researchers selected nanosized material or a higher hydrothermal temperature (usually 150–200 °C) [31,32] to obtain pure $Li_4Ti_5O_{12}$ product. The results here suggest that the impurity of TiO_2 can be eliminated by setting the hydrothermal reaction temperature at 100 °C.

Fig. 1d demonstrates that hydrothermal reaction time also affects the purity of final product. It is clear that the final product obtained by the 5 h reaction time includes the impurity of anatase TiO_2. When the reaction time is extended to 10 h and 15 h, respectively, the intensity of TiO_2 impurity peak is significantly weakened. Pure spinel $Li_4Ti_5O_{12}$ product is obtained when the hydrothermal reaction time is 20 h. It indicates that Li^+ gradually penetrates into the TiO_2 particle as time increases. Therefore, the suitable hydrothermal reaction condition is 100 °C and 20 h for synthesis pure $Li_4Ti_5O_{12}$ product.

3.3. Effect of LiOH solution concentration on $Li_4Ti_5O_{12}$ product

The effects of different concentrations of LiOH solution on the composition of final products are investigated. Fig. 1e demonstrates that the impurity of TiO_2 (anatase and rutile) appears in the final products at the lower concentration of 1 M and 2 M and 800 °C for 2 h. When the concentration of LiOH solution is 5 M, the obtained final product is pure spinel $Li_4Ti_5O_{12}$. It suggests that the high concentration of LiOH solution favors the generation of a homogeneous Li–Ti–O precursor and the precursor easily converts to pure spinel $Li_4Ti_5O_{12}$ after subsequent reaction at 800 °C for 2 h.

The result is different with some previous literatures which used an excessive volume and low concentration of LiOH solution to get homogeneous Li–Ti–O precursors and washed the precursors for a stoichiometric $Li_4Ti_5O_{12}$ product [30–32]. The process is too complicated for mass production. For comparison, the above results suggest that the suitable Li/Ti molar ratio can be obtained by adjusting reaction temperatures or LiOH concentrations to get pure $Li_4Ti_5O_{12}$ product. Our strategy of synthesizing $Li_4Ti_5O_{12}$ product is more facile and efficient for it adopts moderate temperature and no longer needs washing and filtering the precursor.

3.4. TG and FT-IR spectra analysis

Fig. 2 shows the TG curves of the precursors obtained by both hydrothermal (Fig. 2a) and solid-state method (Fig. 2b). In Fig. 2a, the weight loss prior to about 120 °C should be attributed to the removal of a small amount of adsorbed water in the precursor. The continuous weight loss in the temperature range of 150–600 °C can be assigned to the rearrangement reaction of disordered Li in Li–Ti–O precursor to form $Li_4Ti_5O_{12}$ [32]. As can be seen, no weight loss over about 600 °C, suggesting that $Li_4Ti_5O_{12}$ materials can be readily obtained. Besides, the total weight loss during the whole synthesis process is 7.4%, extremely to the theory value of 7.3%. The Fig. 2b is the TG curves of heating the mixture of $LiOH·H_2O$ and TiO_2 obtained by solid-state mechanical mixing. The quick weight loss at near 100 °C should be due to the removal of water of lithium salt in the mixture. The weight loss in the temperature range of 400–600 °C can be assigned to the decomposition of LiOH. And on further heat, $Li_4Ti_5O_{12}$ is formed gradually in this stage. The results above suggest that the homogeneous precursor of TiO_2 and Li–Ti–O is obtained by hydrothermal method.

In order to provide further evidence for the results of TG, The FT-IR spectra of TiO_2, $LiOH·H_2O$, precursor and $Li_4Ti_5O_{12}$ are shown in Fig. 3. The similarity of spectra, including absorption peaks and intensities, shows that there is no significant difference between the absorption of the pristine TiO_2 and the precursor for $Li_4Ti_5O_{12}$, which suggests that the homogeneous precursor of TiO_2 and Li–Ti–O is obtained by the hydrothermal reaction. The process that LiOH solution reacts with TiO_2 might be described as the migration of lithium ion into the micro-structure of TiO_2 to form Li–Ti–O complex. The results above agree well with the XRD and TG analysis. The $Li_4Ti_5O_{12}$ sample has two absorption peaks at 2359.7 cm^{-1} and 668.3 cm^{-1}, which are assigned to the stretching vibration of Ti–O bond and MO_6 (TiO_6) octahedron [24,35]. The absorption bands of C=O at 1622.0 cm^{-1} and –OH at 3429.2 cm^{-1} are detected, which are caused by the strong absorption of CO_2 and H_2O of $Li_4Ti_5O_{12}$ material in the air, respectively [24,36].

3.5. SEM, BET surface area and XRD analysis

As-prepared TiO_2 (sub-micron and micro) with different particle size are used to react with LiOH solution to prepare $Li_4Ti_5O_{12}$. The synthesis condition of all the prepared samples is listed in Table 1. Fig. 4 shows the SEM photos of precursors obtained after the hydrothermal reaction and $Li_4Ti_5O_{12}$ samples. It can be seen from Fig. 4a′–c′ that all the precursors have regular spherical morphology and rough surface. The surface of the final powder is dense and smooth. The regular spherical morphology can ensure a high packing density. The final products have average particle size of 0.3 μm (Fig. 4a), 0.5 μm (Fig. 4b) and 1.0 μm (Fig. 4c), respectively. The corresponding tap densities are 0.85 g cm^{-3}, 0.98 g cm^{-3} and 1.10 g cm^{-3}. The increase of tap density correlates well with the particle size.

The specific surface areas of the synthesized products are shown in Table 1. Sample a shows the highest specific surface area

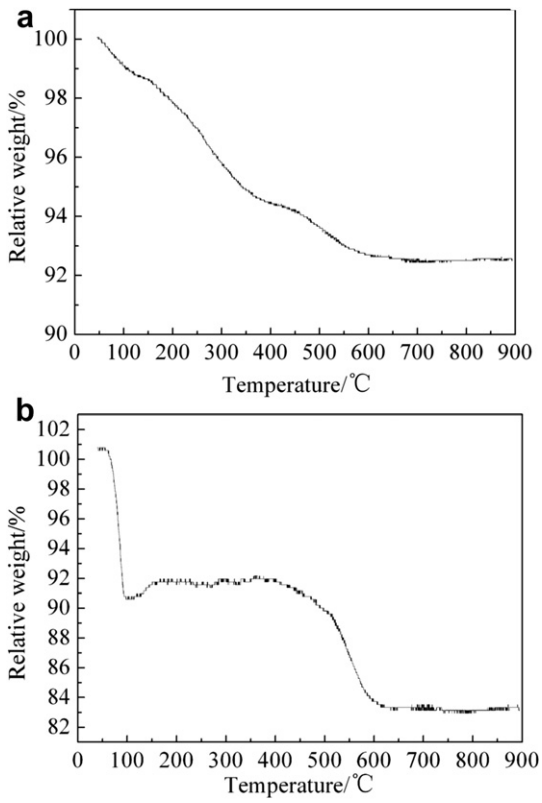

Fig. 2. TG curves of obtained by (a) precursor by hydrothermal method and (b) mechanical mixture of TiO_2 and $LiOH·H_2O$ by solid-state method.

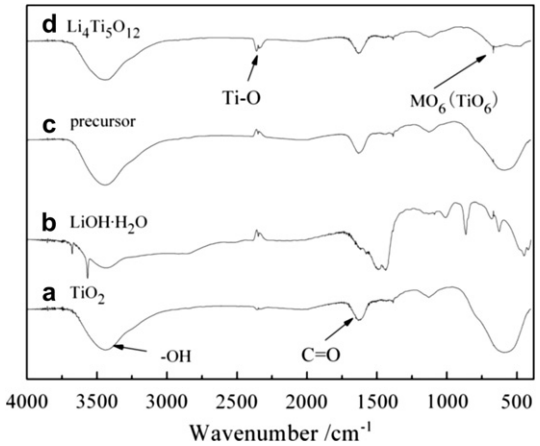

Fig. 3. IR spectroscopy of (a) TiO_2, (b) $LiOH·H_2O$, (c) precursor and (d) $Li_4Ti_5O_{12}$, respectively.

Table 1
Synthesis conditions, particle sizes, specific surface areas and first coulombic efficiencies of three $Li_4Ti_5O_{12}$ samples.

Samples	a	b	c
TiO_2 size (μm)	0.3	0.5	1
Concentration of LiOH (mol L^{-1})	5	5	5
Hydrothermal reaction temperature (°C)	100	100	100
Hydrothermal reaction time (h)	20	20	20
Heat treat temperature (°C)	800	800	800
$Li_4Ti_5O_{12}$ particle size (μm)	0.3	0.5	1
BET (m^2 g^{-1})	6.61	5.80	3.82
Coulombic efficiency (%)	99.9	99.7	100

(6.61 m^2 g^{-1}), while those of samples b and c are 5.80 m^2 g^{-1} and 3.82 m^2 g^{-1}, respectively. Thus, the specific surface areas flow the trend of a (0.3 μm) > b (0.5 μm) > c (1 μm), and smaller particle sizes are associated with higher surface areas. In summary, the results indicate that the pure spinel $Li_4Ti_5O_{12}$ with different particle size and high tap density can be easily obtained by the hydrothermal synthesis method.

The XRD patterns of all the three prepared $Li_4Ti_5O_{12}$ samples are shown in Fig. 5. The diffraction patterns of all the samples are almost identical. The sharp diffraction peaks can be indexed on the

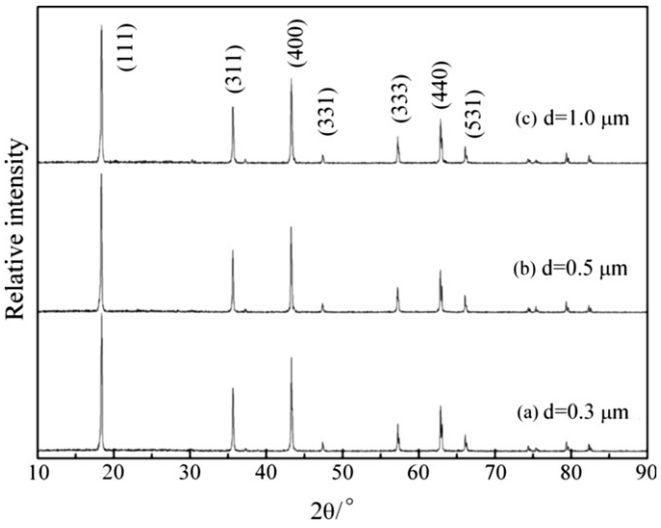

Fig. 5. XRD patterns of as-obtained different particle size $Li_4Ti_5O_{12}$ by the hydrothermal method.

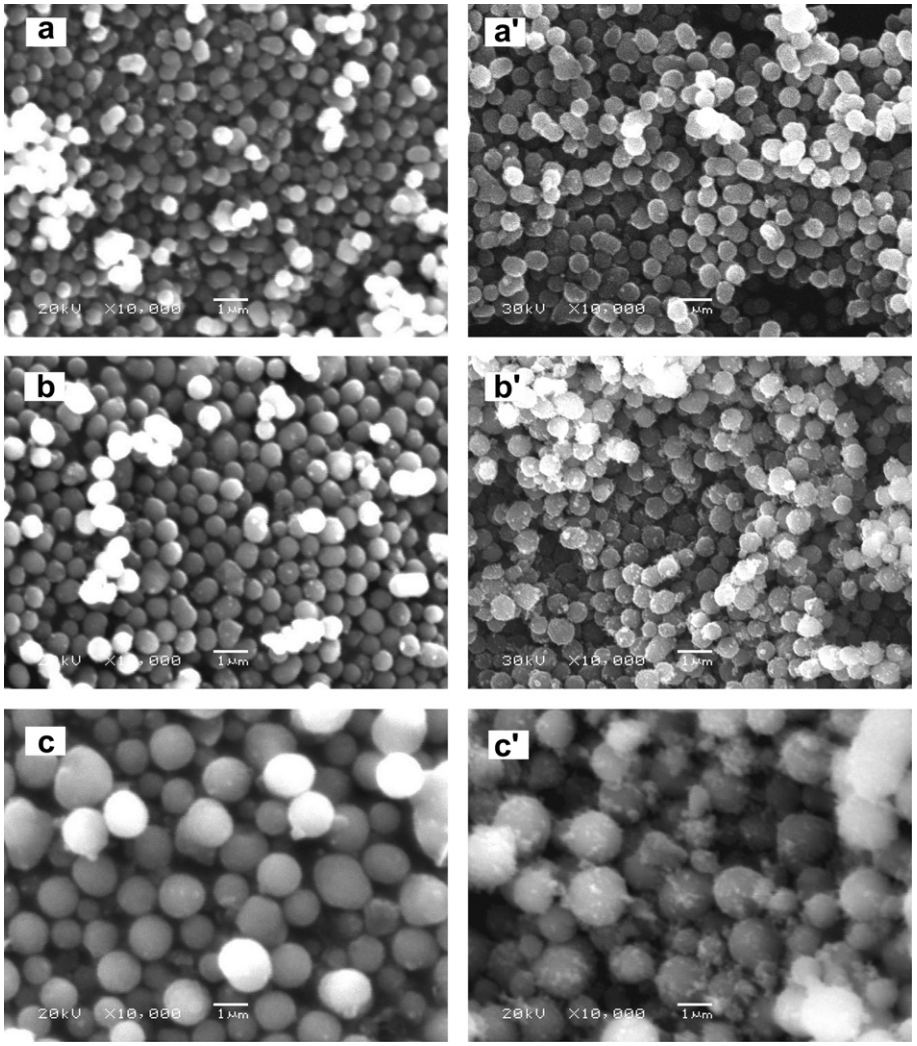

Fig. 4. SEM micrographs of precursors ((a′)–(c′)) obtained after the hydrothermal reaction and the final spherical $Li_4Ti_5O_{12}$ samples with different particle size (a) 0.3 μm, (b) 0.5 μm and (c) 1.0 μm, respectively.

basis of a cubic spinel structure, $Li_4Ti_5O_{12}$ (space group *Fd3m*, JCPDS No. 49-0207). Neither titanium dioxide nor other lithium titanium oxide impurity peaks are detected.

The results indicate that titanium dioxide and lithium hydroxide can be mixed in atomic scale to form a precursor through hydrothermal method, thus the precursor can quickly convert to pure spinel $Li_4Ti_5O_{12}$. Compared to the traditional solid-state synthesis method, in which TiO_2 and $LiOH/Li_2CO_3$ is a non-uniform mixture after ball milling and the subsequent reaction involves long time temperature treatment to ensure diffusion of reactants, the hydrothermal method developed by us is able to form an extremely homogeneous precursor and favor the heat treatment.

3.6. Electrochemical characteristic of $Li_4Ti_5O_{12}$/Li coin-type cell

The electrochemical performances of the $Li_4Ti_5O_{12}$ with three types of particle sizes are investigated at room temperature. The cycling performance for the as-prepared $Li_4Ti_5O_{12}$ electrode at 35 mA g^{-1} in the potential range of 1.0–2.5 V are depicted in Fig. 6A. The 0.5 μm $Li_4Ti_5O_{12}$ (sample b) exhibits the highest capacity among all these samples. The discharge capacity of 159 mAh g^{-1} is maintained after 70 cycles. The capacity of the 1 μm $Li_4Ti_5O_{12}$ (sample a) and 0.3 μm $Li_4Ti_5O_{12}$ (sample c) individually decreases from 146 to 141 mAh g^{-1} and from 139 to 138 mAh g^{-1} after 70 cycles. All the three type samples show excellent cycling stability. Shown in Fig. 6B are the initial charge/discharge curves of the $Li_4Ti_5O_{12}$ electrode in the voltage range of 1.0–2.5 V at 35 mA g^{-1}. It is clear that all these samples have the same discharge plateau at the potential of 1.55 V, which also demonstrates that all samples have pure spinel structure. The coulombic efficiencies of first cycle for the three samples are summarized in Table 1, which shows that all the samples have high coulombic efficiency around 100%.

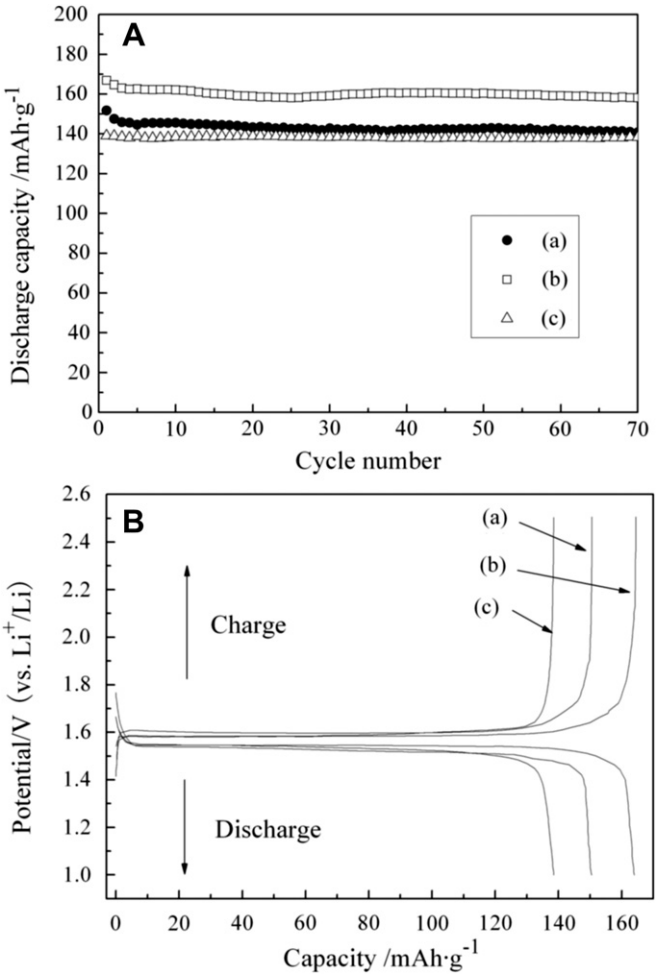

Fig. 6. Cycle performance (A) and initial charge–discharge curves (B) of as-obtained different particle sizes $Li_4Ti_5O_{12}$: (a) 0.3 μm, (b) 0.5 μm and (c) 1.0 μm at 35 mA g^{-1} (0.2 C).

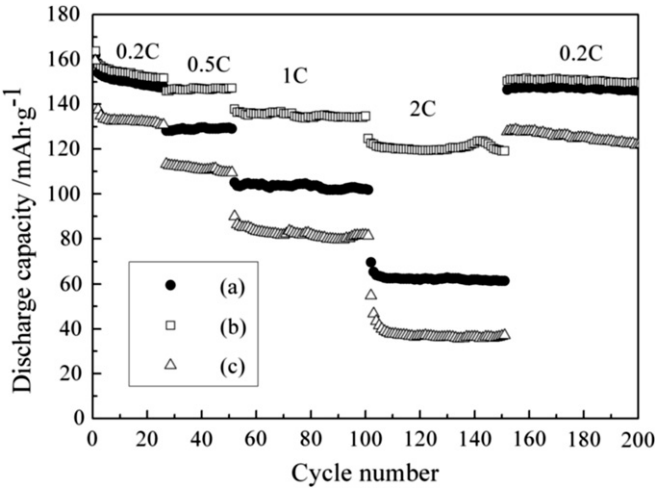

Fig. 7. Capacity versus cycle number at various charge/discharge rates for the synthesized $Li_4Ti_5O_{12}$: (a) 0.3 μm, (b) 0.5 μm and (c) 1.0 μm.

Fig. 7 is the discharge profiles of three samples at various charge/discharge rates from 0.2 C to 2 C. The particle size of samples has significant effect on the discharge capacity. The discharge capacity decreases with increasing current density for all the samples as expected. However, it can be seen from Figs. 6 and 7 that the specific capacity of the cell follows the order of (b) > (a) > (c) at any current rate, which demonstrates that $Li_4Ti_5O_{12}$ particle size of 0.5 μm material shows the best rate performance.

The capacity order of (a) > (c) or (b) > (c) can be understood in terms of the small particle size of the crystallites that leads to increased contact area between the active material and the electrolyte and to decreased Li ion diffusion length [37]. However, the 0.5 μm sample (b) shows better electrochemical properties than 0.3 μm sample (a). This may be because that 0.3 μm sample present

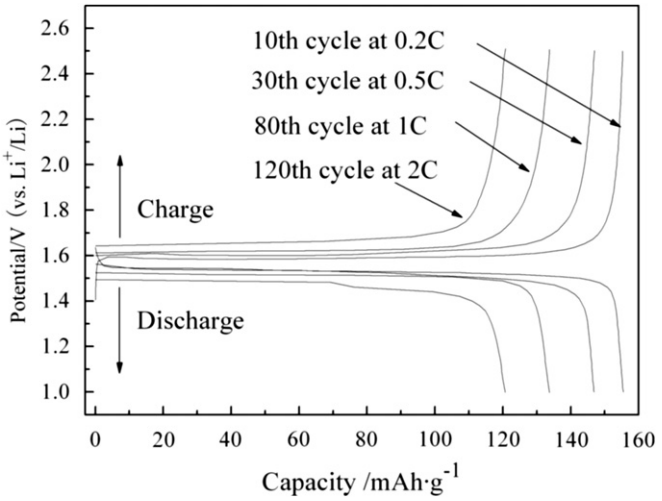

Fig. 8. Charge and discharge curves of $Li_4Ti_5O_{12}$ with the 0.5 μm particle size at various rates.

high specific surface area and greater available reaction sites which stimulates side reactions with electrolyte and leading to the deactivation of the active mass [28]. The chemical stability of $Li_4Ti_5O_{12}$ toward electrolytes should be seriously considered.

The galvanostatic charge and discharge curves of the 0.5 μm $Li_4Ti_5O_{12}$ material at various current densities at different cycle are presented in Fig. 8. At the rate of 0.2 C, the discharge/charge curves display a pair of flat potential plateaus around 1.53 and 1.59 V (vs. Li^+/Li), well corresponding to the two phase equilibrium between two phase, $Li_4Ti_5O_{12}$ and $Li_7Ti_5O_{12}$. Upon the increased rate, the flat potential plateau is maintained, even at the current rate of 2 C. The small potential polarization of as-prepared 0.5 μm material indicates good reaction kinetics, consistent with the excellent high rate capability.

4. Conclusions

In this work, the high tap density and homogeneous particle size distribution (from sub-micron to micro) of pure spinel spherical $Li_4Ti_5O_{12}$ materials are successfully synthesized by a new hydrothermal method. The optimized hydrothermal synthesis condition is that as-prepared anatase TiO_2 reacts with 5 M LiOH solution at 100 °C for 20 h and the obtained precursor is heated at 800 °C for 2 h. Electrochemical measurements demonstrate that the prepared $Li_4Ti_5O_{12}$ with a particle size of 0.5 μm has a stable high charge/discharge capacity and an excellent rate capacity. It delivers 160 mAh g^{-1} at 35 mA g^{-1} (0.2 C) after 70 cycles and 123 mAh g^{-1} at 350 mA g^{-1} (2 C) after 150 cycles. Our hydrothermal method provides a simple and convenient process to prepare $Li_4Ti_5O_{12}$ anode material for Li-ion secondary batteries.

Acknowledgment

This work is supported by National High Technology Research and Development Program of China (863) No. 2008AA11A102.

References

[1] P. An, Qilu, Acta Scientiarum Naturalium Universitatis Pekinensis 42 (2006) 1–7.
[2] R.M. Dell, Solid State Ionics 134 (2000) 139–158.
[3] M. Winter, J.O. Besenhard, M.E. Spahr, P. Novak, Adv. Mater. 10 (1998) 725–763.
[4] J.M. Tarascon, M. Armand, Nature 414 (2001) 359–367.
[5] K. Zaghib, M. Simoneau, M. Armand, M. Gauthier, J. Power Sources 81–82 (1999) 300–305.
[6] K.M. Abraham, D.M. Pasquariello, E.B. Willstaedt, J. Electrochem. Soc. 137 (1990) 743–749.
[7] P. Poizot, S. Laruelle, S. Grugeon, L. Dupont, J.M. Tarascon, Nature 407 (2000) 496–499.
[8] Y. Takeda, M. Nishijima, M. Yamahata, K. Takeda, N. Imanishi, O. Yamamoto, Solid State Ionics 130 (2000) 61–69.
[9] Y.Y. Xia, T. Sakai, T. Fujieda, M. Wada, H. Yoshinaga, J. Electrochem. Soc. 148 (2001) A915–A928.
[10] T. Ohzuku, A. Ueda, N. Yamamoto, J. Electrochem. Soc. 142 (1995) 1431–1435.
[11] T. Yuan, R. Cai, K. Wang, R. Ran, S.M. Liu, Z.P. Shao, Ceram. Int. 35 (2009) 1757–1768.
[12] J. Wang, T.J. Li, Qilu, Acta Phys.-Chim. Sin. (2007) 75–79.
[13] H. Kitaura, A. Hayashi, K. Tadanaga, M. Tatsumisago, J. Power Sources 189 (2009) 145–148.
[14] J.L. Allen, T.R. Jow, J. Wolfenstine, J. Power Sources 159 (2006) 1340–1345.
[15] K. Naoi, S. Ishimoto, Y. Isobe, S. Aoyagi, J. Power Sources 195 (2010) 6250–6254.
[16] K. Zaghib, M. Armand, M. Gauthier, J. Electrochem. Soc. 145 (1998) 3135–3140.
[17] S. Scharner, W. Weppner, P. Schmid-Beurmann, J. Electrochem. Soc. 146 (1999) 857–861.
[18] S.I. Pyun, S.W. Kim, H.C. Shin, J. Power Sources 81–82 (1999) 248–254.
[19] A. Guerfia, S. Sevigny, M. Lagace, P. Hovington, K. Kinoshita, K. Zaghib, J. Power Sources 119–121 (2003) 88–94.
[20] M. Venkateswarlu, C.H. Chen, J.S. Do, C.W. Lin, T.C. Chou, B.J. Hwang, J. Power Sources 146 (2005) 204–208.
[21] D. Wang, N. Ding, X.H. Song, C.H. Chen, J. Mater. Sci. 44 (2009) 198–203.
[22] S. Bach, J.P. Pereira-Ramos, N. Baffier, J. Power Sources 81–82 (1999) 273–276.
[23] C.H. Jiang, M. Ichihara, I. Honma, H.S. Zhou, Electrochim. Acta 52 (2007) 6470–6475.
[24] Y. Li, H.L. Zhao, Z.H. Tian, W.H. Qiu, X. Li, J. Alloys Compd. 455 (2008) 471–474.
[25] Y. Yu, J.L. Shui, C.H. Chen, Solid State Commun. 135 (2005) 485–489.
[26] K. Nakahara, R. Nakajima, T. Matsushima, H. Majima, J. Power Sources 117 (2003) 131–136.
[27] A.D. Pasquier, C.C. Huang, T. Spitler, J. Power Sources 186 (2009) 508–514.
[28] A.S. Arico, P. Bruce, B. Scrosati, J.M. Tarascon, W. van Schalkwijk, Nat. Mater. 4 (2005) 366–377.
[29] K. Amine, I. Belharouak, Z. Chen, T. Tran, H. Yumoto, N. Ota, S.T. Myung, Y.K. Sun, Adv. Mater. 22 (2010) 3052–3057.
[30] Y.S. Lin, J.G. Duh, J. Power Sources 196 (2011) 10698–10703.
[31] C.H. Jiang, E. Hosono, M. Ichihara, I. Honma, H.S. Zhou, J. Electrochem. Soc. 155 (2008) A553–A556.
[32] D. Fattakhova, V. Petrykin, J. Brus, T. Kostlanova, J. Dedeek, P. Krtil, Solid State Ionics 176 (2005) 1877–1885.
[33] H. Yan, H. Zhang, D. Zhang, Z. Zhu, Qilu, Acta Phys.-Chim. Sin. 27 (2011) 2118–2122.
[34] D. Fattakhova, P. Krtil, J. Electrochem. Soc. 149 (2002) A1224–A1229.
[35] G.C. Allen, M. Paul, Appl. Spectrosc. 49 (1995) 451–458.
[36] L. Gao, J.Y. Chen, J.H. Huang, D.S. Yan, J. Inorg. Mater. 10 (1995) 421–427.
[37] P.G. Bruce, B. Scrosati, J.-M. Tarascon, Angew. Chem. Int. Ed. 47 (2008) 2930–2946.